JOURNAL OF CATALYSIS 139, 551–560 (1993)

Catalyst Characterization Using Quantitative FTIR: CO on Supported Rh

P. B. RASBAND AND W. C. HECKER

BYU Catalysis Laboratory, Department of Chemical Engineering, 350 CB, Brigham Young University, Provo, Utah 84602

Received May 4, 1992; revised September 9, 1992

Qualitative FTIR has been and continues to be one of the most utilized tools in the characterization of supported metal catalysts. *Quantitative* FTIR has the potential to allow catalysis researchers to determine the surface concentrations of active intermediates. However, its successful application depends upon an understanding of the factors affecting integrated absorption intensities (coefficients relating IR absorbance to surface concentration). This work addresses the effect of metal particle size and temperature on the absorption intensities for CO chemisorbed on Rh/SiO_2. Absorption intensities for both linear and bridged CO surface species (A_l and A_b) were determined by combining peak area data from IR spectra with uptake measurements obtained in gravimetric experiments. This resulted in an A_l value of 13 (±2) and an A_b value of 42 (±6) cm/μmol. No statistically significant particle size effect has been observed for average spherical particle diameters ranging from 13 to 58 angstroms (100 to 22% dispersion). Also, integrated absorption intensities for linear and bridged CO were shown to vary little over the temperature range of 323 to 473 K. The discovery that absorption intensities determined for one temperature and metal dispersion may be used for other temperatures and dispersions is a welcome result which may broaden the application of quantitative FTIR. Rh dispersions were determined for Rh/SiO_2 samples of five different weight loadings using the absorption intensities determined in this study. The variation of Rh dispersion with Rh loading was practically identical to that observed in hydrogen chemisorption experiments conducted on another series of Rh/SiO_2 catalysts. Also, it was observed that the ratio of linear to bridged CO surface concentrations increased from 2 to 5 as Rh dispersion increased from 22 to 100%. These observations demonstrate the usefulness of a more fully developed quantitative FTIR technique.

INTRODUCTION

Although FTIR is most often thought of as a *qualitative* tool useful in identifying species present during surface reactions, it can also be used under certain circumstances as a means of determining surface concentrations. Primet *et al.* (*1*) have used quantitative IR spectroscopy in the determination of metal dispersion in Pt/Nb_2O_5 and Pt/CeO_2 catalysts for which hydrogen–oxygen titration methods are not suited. Hecker *et al.* (*2*) used chemisorbed CO as a quantitative probe in studying the type and number of surface sites in molybdena- and ceria-modified Rh/SiO_2 catalysts for the reduction of NO by CO. This method has also been used to study $Rh/Nb_2O_5/SiO_2$ catalysts for the same reaction (*3*). Other examples of applied quantitative FTIR for chemisorbed CO have been published by Kaul and Wolf (*4*), Yokomizo *et al.* (*5*), and Winslow and Bell (*6*).

The relation most often used to relate CO surface concentration to IR peak areas is the integrated Beer–Lambert relation (*7–9*):

$$a_i = A_i L C_i. \qquad (1)$$

In this relation, i represents a specific surface species (e.g., linear CO), a_i is the area under the IR absorbance peak attributed to species i (units of cm^{-1}), L is the sample thickness or path length, and C_i is concentration of i (units of $\mu mol/cm^3$). A_i is the *integrated absorption intensity* (units of cm/μmol) and can be thought of as an extinction

0021-9517/93 $5.00

coefficient averaged over the absorbance peak for i. When using absorption intensities, care must be taken to avoid confusion between ln-based and $\log_{10}$-based absorbance. Equation (2) is an unambiguous definition of the absorption intensity used throughout this work:

$$A_i = a_i/LC_i = (1/LC_i)\int_{\nu_1}^{\nu_2} \log_{10}(T_0/T)d\nu. \quad (2)$$

Here, T/T_0 is the fraction of the radiant energy transmitted through the sample and ν is the frequency in cm^{-1}.

Another form of the integrated Beer–Lambert relation can be easily derived (*3*) which is more convenient for solid samples in pressed wafer form (Eq. (3)). If A_c and m are the cross-sectional area and mass of the wafer, respectively, and n_i is the molar uptake of species i (μmol i/g), then the moles of surface species i in the sample wafer can be expressed as either A_cLC_i or mn_i. Equating these two expressions, solving for LC_i, and substituting the result into Eq. (1) gives

$$A_in_i = a_iA_c/m. \quad (3)$$

Thus, the value of n_i (and therefore the surface concentration of i) can be determined from Eq. (3), the IR spectrum, and the physical properties of the catalyst wafer *if the A_i value is known*. Hence, the development of a quantitative FTIR tool has been reduced to the problem of obtaining values for the integrated absorption intensity, A_i, for each surface species i, and as a function of potentially important factors such as metal, metal crystallite size, coverage, temperature, and so on.

A very limited amount of data has been collected on absorption intensities. Seanor and Amberg (*8*) calibrated the IR spectra of linear CO on Pt/SiO_2, Cu/SiO_2, and several other samples through simultaneous gravimetric and IR experiments. One of the first studies to determine separate absorption intensities for linear (high-frequency) and bridged (low-frequency) CO simultaneously adsorbed on a metal surface was conducted by Vannice and co-workers (*9, 10*). They studied Pt and Pd on several supporting oxides. Duncan *et al.* (*11*) used C^{13} NMR to calibrate IR spectra of CO chemisorbed on 2.2% Rh/Al_2O_3 samples. Their research was perhaps the very first work to determine separate absorption intensities for linear, bridged, and geminal (dicarbonyl) CO on a metal surface. Cant and Donaldson (*12*) used Pt/SiO_2 samples to investigate the effect of metal particle size on the position and shape of IR bands from linear CO and determined that a small decrease in A_l occured as the Pt loading (and presumably Pt particle size according to Cant and Donaldson) was increased. However, the observed changes were very small, barely outside the estimated experimental error. Shigeishi and King (*13*) investigated, among other factors, the variability of integrated absorption intensity with surface coverage, θ_{CO}. They noted that for a saturated surface, the value of A_l on Pt{111} was 12.8 cm/μmol (based on $\log_{10}$ rather than $\log_e$). According to their findings, A is a complex function of θ_{CO}. Finally, Cavanagh and Yates (*14*) conducted a study from which they concluded that the geminal CO absorption intensity, A_g, was essentially independent of coverage for a 0.2% Rh/Al_2O_3 sample.

Most of the previous absorption intensity studies have largely ignored the effects of metal particle size (or dispersion) and temperature. The investigation described in this paper attempts to elucidate the temperature and dispersion effects on the values of the integrated absorption intensity for linear, bridged, and geminal CO chemisorbed on Rh/SiO_2. It is hoped that such knowledge will broaden the applicability of quantitative FTIR in the study of catalytic materials.

EXPERIMENTAL METHODS

Approach. Experimental determination of absorption intensities requires an independent method of measuring the amount of each species i (n_i) on the surface. Gravimetric experiments can be performed which

give the *total* amount of CO on the supported Rh surfaces: linear, bridged, and geminal CO. In such a case, the mass balance can be written as

$$n_l + n_b + n_g = n_{tot}. \quad (4)$$

Equation (4) can be modified slightly to include the integrated absorption intensities and written

$$(A_l n_l)/A_l + (A_b n_b)/A_b + (A_g n_g)/A_g = n_{tot}. \quad (5)$$

As shown in Eq. (3), the numerators in each of the three terms on the left hand side of Eq. (5) can be determined from FTIR spectra, and from the mass and dimensions of the catalyst wafer. Therefore, the only variables in Eq. (5) which remain unknown are the denominators (absorption intensities).

Equation (5) provides one relation in the unknowns A_l, A_b, and A_g. Results from Duncan *et al.* (*11*) can be used with a simple assumption to provide an additional relation in A_l and A_b. For ^{13}CO chemisorbed on 2.2% Rh/Al_2O_3 values of 11.3 and 36.9 cm/μmol were determined for A_l and A_b, respectively. If it is *assumed* that the ratio A_l/A_b is not dependent upon the carbon mass or the support material, then the ratio of A_l to A_b for the experiments in the current work is known. (The validity of this assumption for our particular experimental conditions can be determined after considering the results.)

$$(A_l/A_b)_{12,silica} = (A_l/A_b)_{13,alumina} = 11.3/36.9 = 0.306. \quad (6)$$

The geminal intensity, A_g, can be crudely estimated through thermal desorption experiments. Since geminal CO is weakly chemisorbed relative to linear and bridged CO (*15*), a small temperature range ought to exist at a relatively low temperature over which the equilibrium coverage of geminal CO varies, while the linear and bridged CO remain essentially at full coverage. Within this temperature range changes in sample mass with temperature allow the direct calculation of n_g and hence A_g.

Samples. In order to obtain samples with varying Rh particle size, Rh/SiO_2 samples of (nominally) 0.2, 0.6, 2.0, 6.0, and 9.0 wt% Rh were prepared using the incipient wetness technique. Three replicates of each loading were made for a total of fifteen preparations. The Cab-o-sil M-5 silica was saturated with an aqueous solution of $RhCl_3 \cdot 3H_2O$ (Alfa Products, Thiokol Corp.), dried for 12 h at 353 K, and then calcined in air at 773 K for 4 h.

Experimental design, procedures, and equipment. Total CO uptake, n_{tot}, was determined for each of the fifteen samples using a Perkin–Elmer TGA-7 thermogravimetric analyzer (sensitivity of 1 μg). Samples were pressed into wafers on an hydraulic press (in order to more closely match conditions found in the infrared experiments) and fragmented. Pieces of approximately 10 mg were used in the gravimetric experiments. After loading, samples were reduced at 473 K for 3 h and cooled to 323 K in H_2 at a flowrate of 200 sccm (cm^3 (STP)/min). Following a 5-min He purge, CO adsorption was begun in a stream of 2% CO/He at 200 sccm and approximately 1 atm total pressure. The CO adsorption was carried out for 30 min before final gravimetric or FTIR data were recorded. (During the final 15 to 20 min of that half-hour period, spectra demonstrated peaks of constant size and shape, and the mass measured in the gravimetric experiments was also constant. Hence, it is believed that when final data were recorded, CO was adsorbed at an equilibrium coverage evenly through the wafer.)

FTIR spectra were obtained on a Nicolet 730 spectrometer. The IR signal was collected by a liquid-N_2-cooled photoelectric detector. Frequency resolution was 4 cm^{-1} for the 50 background and 50 sample scans. The sample cell used in these FTIR experiments is very similar to one described by Hicks *et al.* (*16*) and is described in detail elsewhere (*3, 17*). Reduction and adsorption conditions in the infrared experiments were identical to those used in the gravimetric experiments.

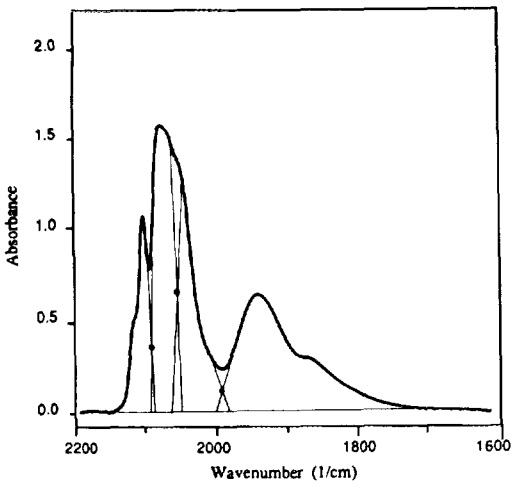

FIG. 1. Example of peak resolution method.

H_2 and He feed gases were passed through O_2-absorbing traps (Alltech Corp.) and desiccant/5A molecular sieve columns (Matheson) before being sent to the gravimetric or FTIR cell. The CO feed was cleansed of carbonyl impurities by passing it through a 5A molecular sieve column maintained at 493 K.

The FTIR and gravimetric experiments described above were carried out in a random order to minimize the effect of external, unknown factors. Sample preparation order was also randomized.

IR peak resolution. In order to assign peak areas, a_i, to each band for use in Eq. (3), it is necessary to isolate the *individual* IR peaks which combine to give the spectrum trace observed in the FTIR experiment. This isolation of IR peaks is referred to as "peak resolution." Figure 1 shows the extensive overlap of IR peaks associated with the various CO species typically observed on the Rh surface. Peak resolution, in practice, amounts to finding (approximations to) the hidden components of each peak in the spectrum. Once this is done, the individual peaks can be analyzed to determine peak areas, a_i.

In this work a graphical method of spectrum resolution was used. First, each peak in the spectrum was identified. In some cases adjacent peaks shared only a small amount of common area, in which case a local minimum in the spectrum between the adjacent peaks was observed. In other cases a much greater overlap was observed and the local minimum was replaced with a point of inflection in the spectrum trace. Next the spectrum baseline was drawn. This was usually very close to the horizontal line passing through the zero on the absorbance axis. Following this, "midpoints" were located halfway between each local minimum (or inflection point) and the baseline directly below. (This peak resolution method assumes that this mid-point occurs at a vibrational frequency where both peaks are contributing equally to the observed spectrum trace.) Finally, through each midpoint two lines are drawn, one tangent to the right-hand peak and one tangent to the left-hand peak. The points at which these lines meet the spectrum trace will usually be near the top of the peak where absorbance contributions from the opposite peak are at a minimum. The lines are approximations to the peaks' hidden components. Also, if the pair of lines through a given midpoint have been correctly placed, the small "triangle" between the midpoint and trace will have an area approximately equal to that of the triangle between the midpoint and the baseline. Examples of applications of this resolution method can be found in Rasband (*17*).

RESULTS AND DISCUSSION

Absorption intensity with varying Rh particle size. Figure 2 shows a typical spectrum of CO on a supported Rh surface. The tallest peak at about 2080 cm^{-1} is assigned (*18*) to linear CO (one CO molecule adsorbed on a single Rh atom). The peaks at about 2040 and 2100 cm^{-1} are associated with the antisymmetric and symmetric vibrations for geminal (dicarbonyl) CO (*18*). The high-frequency geminal peak has an upper shoulder arising from the *P* branch of the gaseous CO vibrational–rotational spectrum. The CO_g peak is centered at about 2140 cm^{-1}

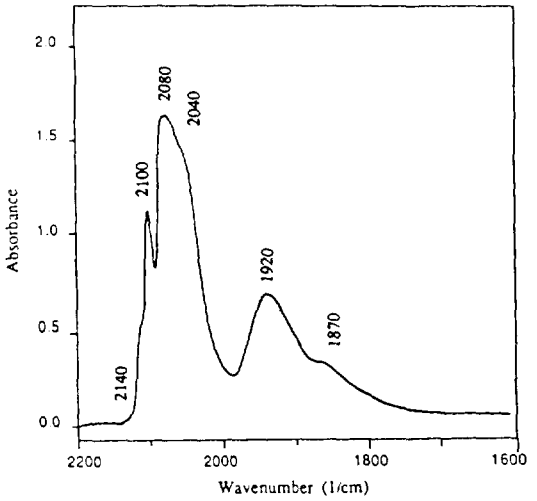

FIG. 2. Spectrum of CO chemisorbed on a 6.0 wt% Rh/SiO_2 sample at 323 K.

and the *R* branch is between 2140 and 2200 cm^{-1}. It is also possible that the shoulder on the geminal peak is due to CO on an oxidized Rh site (*18*). The area under this shoulder was too small to determine with good accuracy so its contribution to the upper geminal CO peak area was ignored. (The resulting error in the estimate of the geminal absorption intensity is much smaller than the precision of the A_g estimate.) The two large peaks below 2000 cm^{-1} come from bridged CO surface species. The peak at about 1870 cm^{-1} was assigned to a 1:2 CO–Rh species and the peak at 1920 cm^{-1} was assigned to a 3:2 stoichiometry (*18*).

As required by Eq. (3), the areas under each IR peak (a_i) for each Rh loading were determined by integration and then multiplied by the wafer cross-sectional area (4.91 cm^2) and divided by the wafer mass which varied from 0.15 to 0.25 g. These normalized area values are shown in Table 1. Each number represents the average of three results and the number in parentheses are the standard deviations. Note that the two bridged peaks have been lumped together, as have the two geminal CO peaks.

Figure 3 shows the total uptake of CO, n_{tot}, for each Rh loading determined through

TABLE 1

Normalized Peak Areas from FTIR Spectra (a_iA_c/m)

Rh loading (wt%)	a_iA_c/m in cm/g (std. dev.)		
	Linear	Bridged	Geminal
0.2	173 (27)	121 (81)	197 (99)
0.6	481 (73)	287 (37)	358 (49)
2.0	835 (102)	617 (104)	571 (64)
6.0	1249 (56)	1877 (297)	1677 (201)
9.0	1511 (375)	2454 (226)	1717 (165)

the gravimetric experiments. Standard deviations are indicated by the error bars. Note that the smooth curve through the points extrapolates to 0% Rh at a point around 10 or 20 μmol/g rather than the origin as would be expected. During the 5-min He purge immediately following reduction and cooling and just prior to CO adsorption, a very gradual increase in sample mass was observed. While efforts to eliminate this problem failed, special blank experiments performed on the TGA apparatus demonstrated that the weight increase continued over a 30-min He purge and was more than twice that corresponding to the complete oxidation of all the Rh to Rh_2O_3 for the 0.2% sample. The increase was also observed to be independent of the Rh loading in the sample. Also, the unexpected mass gain did not ap-

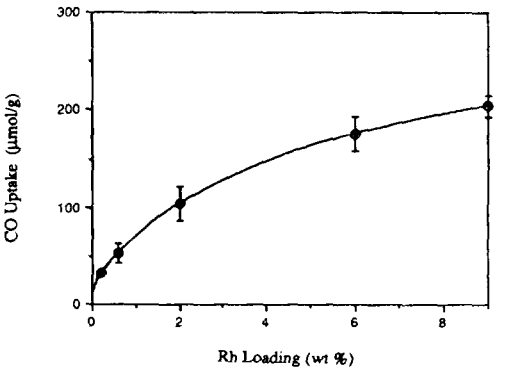

FIG. 3. Total CO uptake vs Rh loading as determined through gravimetric experiments.

TABLE 2

Unadjusted Absorption Intensities (A_i), Surface Species Concentrations (n_i), and Rh Dispersions as a Function of Rh Loading

Rh (%)	A_i (cm/μmol)		n_i (μmol/g)			Dispersion (%)
	Linear	Bridged	Linear	Bridged	Geminal	
0.2	6.7	22.4	25.8	5.4	1.5	167
0.6	11.3	37.6	42.6	7.6	2.8	88
2.0	10.3	34.3	81.1	18.0	4.4	52
6.0	11.2	37.2	112.	50.4	13.	28
9.0	11.8	39.3	128.	62.6	13.	22

pear until the sample temperature had dropped below approximately 340 or 350 K. This problem of the unexpected mass gain required a slight adjustment in the gravimetric data which will be described and further justified later.

The thermal desorption FTIR and gravimetric experiments were conducted as described above to determine the absorption intensity for geminal CO. These were performed at 373 K and resulted in an estimate of A_g = 130 cm/μmol. These experiments demonstrated fairly poor reproducibility and, hence, a large uncertainty (approximately 50 cm/μmol) is associated with this result. However, as will be demonstrated shortly, this large uncertainty in A_g *does not* lead to large uncertainties in the values of A_l and A_b.

Given the estimate for A_g and the working assumption that $A_l/A_b = 0.3$, the results in Table 1 and Fig. 3 can be combined using Eq. (5) to obtain the absorption intensity estimates shown in Table 2. Once the A_i values were known, the numbers of linear, bridged, and geminal sites (n_i) for each Rh loading could be determined from the data in Table 1 and the relationship in Eq. (3). In calculating the number of bridged sites it was assumed that roughly equal amounts of 3 : 2 and 1 : 2 bridged CO were present, giving an average CO/Rh ratio of 1. The linear CO ratio is also 1, and the geminal CO ratio is 2. Knowing the numbers of sites makes it a simple matter to estimate the Rh dispersion (ratio of surface Rh atoms to total Rh atoms) if it is assumed that the equilibrium coverage of CO corresponded to full coverage. These dispersion values along with the values of n_i are shown in Table 2.

A plot of the dispersion results as a function of Rh loading is shown in Fig. 4. Also shown are results from Hecker and Breneman (*19*) which were obtained on a different series of Rh/SiO_2 samples using hydrogen uptake measurements taken in a glass vacuum apparatus. The two curves show remarakble agreement. Figure 4 supports the conclusion that the 0.2% Rh samples used in this study are essentially 100% dispersed. The difference between 100% and 167% dispersion for the lowest Rh loading amounts to 13 μmol/g in total CO uptake. This is very close to the discrepancy of 10 to 20 μmol/g noted above in the gravimetric results of Fig. 3. Therefore, although a definitive identification of the causes of the unexpected weight gain has not been made, it seems reasonable to make an adjustment in the baseline of the gravimetric data (i.e., subtract 13 μmol/g from each result). This adjustment results in the absorption intensities, surface species concentrations, and dispersions shown in Table 3. Note that, in contrast to Table 2, where the absorption intensities vary significantly with Rh loading, these shown in Table 3 are essentially

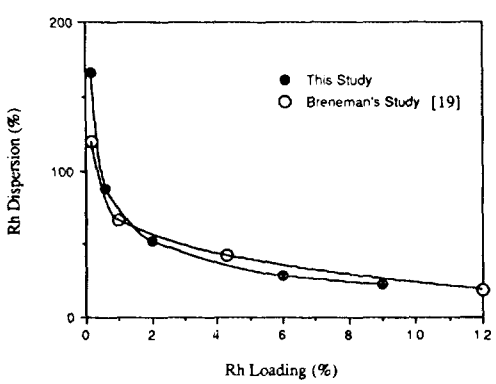

FIG. 4. Dispersion estimates for Rh/SiO_2 samples as determined through quantitative FTIR (this work) and hydrogen chemisorption (*19*).

TABLE 3

Adjusted Absorption Intensities (A_i), Surface Species Concentrations (n_i), and Rh Dispersions as a Function of Rh Loading

Rh (%)	A_i (cm/μmol)		n_i (μmol/g)			Dispersion (%)
	Linear	Bridged	Linear	Bridged	Geminal	
0.2	11.7	39.0	14.8	3.1	1.5	100
0.6	15.5	51.5	31.1	5.6	2.8	68
2.0	11.9	39.6	70.2	15.6	4.4	46
6.0	12.1	40.3	103.	46.3	13.	28
9.0	12.6	42.0	120.	58.3	13.	22

independent of Rh loading. These values are 13 (±2) cm/μmol for A_l and 42 (±6) cm/μmol for A_b. Note also from the data in Table 3 that the ratio of the surface concentrations of bridged CO to linear CO increased from 0.2 to 0.5 as Rh dispersion decreased from 100 to 22%. There are no definite trends in the ratio of geminal to linear CO.

Linear and bridged integrated absorption intensities have been plotted vs Rh loading in Fig. 5. The error bars show the standard deviations. Regression lines are also included and show again that A_l and A_b are essentially independent of Rh particle size. Also note that the values of A_l and A_b (13 and 42 cm/μmol, respectively) are, within experimental error, equal to those determined by Duncan *et al.* (*11*) (11.3 and 36.9 cm/μmol) for ^{13}CO on Rh/Al_2O_3. This agreement supports the assumption regarding the linear-to-bridged intensity ratio (A_l/A_b = 0.3).

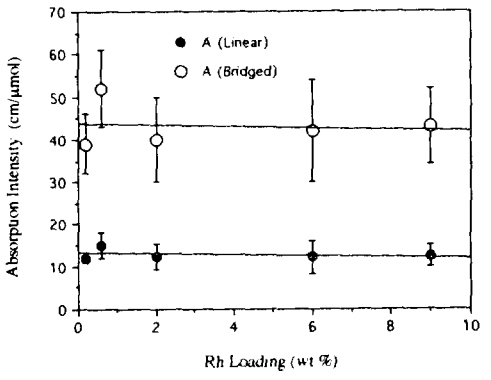

FIG. 5. Linear and bridged absorption intensities vs Rh loading (323 K).

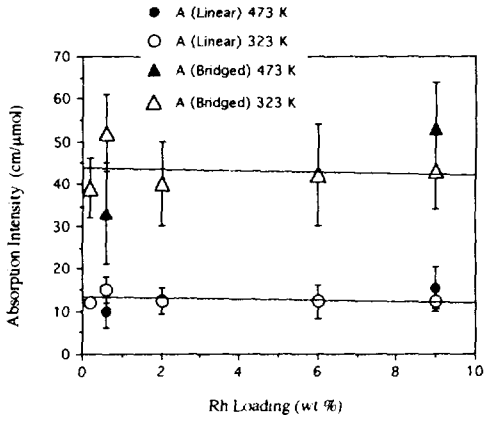

FIG. 6. Linear and bridged absorption intensities at 473 and 323 K.

It was noted above that the estimate for A_g contains a large amount of uncertainty. The question regarding the sensitivity of the A_l and A_b results to the error in A_g must be addressed. The calculations of the linear and bridged absorption intensities were repeated using a value of 65 cm/μmol rather than 130 cm/μmol for A_g. Halving the absorption intensity doubled the estimate of geminal CO on the Rh surface. However, since this still resulted in a relatively small amount of geminal CO relative to the amount of linear and bridged CO, the estimates of A_l and A_b changed little (about 4%).

Absorption intensity with varying temperature. To determine whether adsorption intensities for chemisorbed CO are a function of temperature, FTIR and gravimetric experiments similar to those described above were repeated at 473 K rather than 323 K. Rather than using only one Rh loading in these temperature sensitivity experiments, two (extreme) loadings were used. The resulting absorption intensity values for linear and bridged CO on 0.6 and 9.0% Rh are shown in Fig. 6 with standard deviations included (based on three replications at each

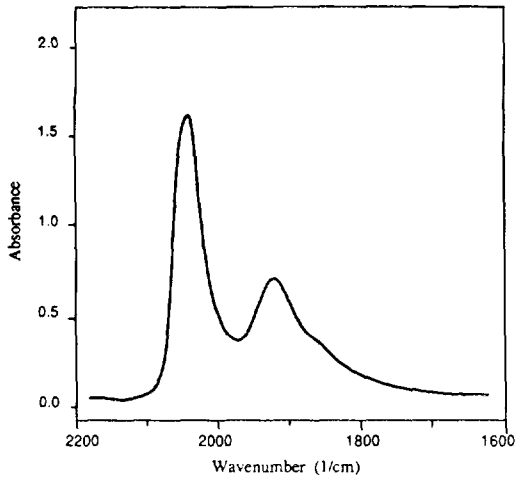

FIG. 7. Spectrum of CO chemisorbed on a 9.0 wt% Rh/SiO_2 sample at 473 K.

loading). It can be seen that at both Rh loading extremes, both linear and bridged CO demonstrate no variation of absorption intensity with temperature outside the limits of confidence in the data.

Figure 7 shows the high-temperature (473 K) spectra for one of the 9% Rh catalysts. Note that the positions and shapes of the linear and bridged CO peaks are not greatly affected by the 150° temperature increase, although there is a slight shift to the right (approx. 20 cm^{-1}) in the linear band's peak position. This shift could be due to a slight decrease in CO coverage which, according to the work of Winslow and Bell on Ru/silica (*6*), would translate to an approximate decrease in the value of the linear adsorption intensity of 10 to 20%. This discrepancy is still within the error bounds seen in Fig. 6, however. The main difference between the spectra in Fig. 7 and those for the same catalyst taken at 323 K is the disappearance of the bands attributable to the gem-dicarbonyl species in the high-temperature spectrum. This species is generally thought to be less stable than the linear or bridged species, however, so it is not surprising that it would disappear first.

Absorption intensity with varying substrate metal. In order to generalize the application of quantitative FTIR using chemisorbed CO to other catalyst systems besides Rh, it will be necessary ultimately to determine the effect of metal type on integrated absorption intensities. While more data will undoubtedly be needed to make such a determination, it may be constructive to consider here the results of this research in the context of previously published results. Table 4 summarizes most of the published values of absorption intensities ($\log_{10}$ based) for linear CO on several metals. The table also contains values of the dipole moment derivative $d\mu/dr_{co}$ calculated from (8)

$$A = (N_0\pi/6.909\ c^2 m_r)(d\mu/dr_{co})^2 \quad (7)$$

In this relation, r_{co} is the distance between the oxygen and carbon nuclei, μ is the electric dipole moment on the entire M–C–O system (where M represents the collection of metal atoms in the solid), m_r is the reduced mass of the vibrating system, c is the speed of light, and N_0 is Avogadro's number. Relating absorption intensity values to the dipole moment derivative can give physical significance to the absorption intensity and aid in interpreting experimental data.

Variations in dipole moment derivatives can be rationalized upon consideration of the CO–metal bond. Since its introduction in 1965, the Blyholder model for chemisorbed CO (*20*) has been used successfully to explain many spectral characteristics of CO on metal surfaces. Molecular orbital theory (*7*) predicts that gas phase CO would have one filled σ-bonding orbital, two filled π-bonding orbitals, one empty σ-antibonding orbital, and two empty π-antibonding orbitals. Also, the carbon and oxygen atoms have filled valent atomic s-orbitals which participate relatively little in the CO bond. In the Blyholder model the s and p_z atomic orbitals on carbon hybridize so that one sp_z electron forms the σ bond with the electron from the oxygen p_z orbital and the other sp_z orbital contains a pair of electrons which can form a σ coordinate bond with an empty

TABLE 4

Values of Linear Absorption Intensity (A_1) and Dipole Moment Derivatives with Respect to C–O Bond Length ($d\mu/dr_{co}$) for CO Chemisorbed on Several Metals

Metal	A_1 (cm/μmol)	$d\mu/dr_{co}$ (D/A)	Origin	Ref.
Rh	11.3	6.5	Dunc./Yates/Vau.	(*11*)
	12.5	6.8	Rasband/Hecker	(This work)
Pt	12.6	6.9	Shigeishi/King	(*13*)
	14	7.2	Seanor/Amberg	(*8*)
	18.7	8.4	Cant/Donaldson	(*12*)
	22	9.1	Cant/Donaldson	(*12*)
	39	12.1	Vannice/Twu	(*9*)
	43	12.7	Vannice/Twu	(*9*)
Pd	6.1	4.8	Vannice/Wang	(*10*)
	8.2	5.5	Vannice/Wang	(*10*)
	29	10.4	Vannice/Wang	(*10*)
Cu	3	3.3	Seanor/Amberg	(*8*)
	23	9.3	Seanor/Amberg	(*8*)

d orbital on the metal surface. However, since the donation of electrons into the metal atom gives it a partial negative charge, it relieves some of this stress by donating charge from metal d orbitals to the π-antibonding orbitals of the CO group (forming the "back-bond").

Note that both donations (the σ donation from CO to the metal and the π donation from the metal back to the CO molecule) weaken *and lengthen* the C–O bond resulting in lower vibration frequency for chemisorbed CO relative to gas phase CO. According to the literature (*8*, *21*, *22*) the longer C–O bond also results in higher values for $d\mu/dr$ and hence absorption intensity. Blyholder concluded that the back-donation was much more important in determining the C–O bond strength than the carbon-to-metal donation. However, more detailed ab initio calculations on a Ni–C–O system (*23*) have shown that the back-bonding donation may not be as dominating as previously believed.

This view of CO–metal bonding suggests that metals with different electronegativities should lead to different extents of donation and back-donation for a carbonyl system. A metal with a high electronegativity should draw electrons strongly from the carbon in the σ bond (coordination bond) and push electrons weakly into the back-bond in relation to the behavior of a less electronegative metal. Thus, if the σ bond is more important than the back-bond in determining the C–O bond length and absorption intensity, then the highly electronegative metal will lead to a longer C–O bond and a larger value for A. Much more data for CO on a wider variety of metals will be required before these ideas can be evaluated. However, the value of understanding the effect of metal type on integrated absorption intensity would be so great that it would almost certainly justify the great effort required to collect that data.

CONCLUSIONS

Several conclusions can be drawn from the work completed: (i) The integrated absorption intensity for linearly bonded CO on Rh/SiO_2 is 13 ($\pm$2) cm/μmol and that of bridge-bonded CO is 42 ($\pm$6) cm/μmol. A crude estimate of the geminal absorption intensity on the Rh/SiO_2 samples is 130 ($\pm$50) cm/μmol. (ii) No statistically significant Rh dispersion effect has been observed. Any dispersion effect which may exist is very small and can probably be ignored in quantitative FTIR applications. (iii) Although temperature may exert some effect on the ab-

sorption intensity values, the effect is not large. Between 323 and 473 K no effect was observed which would satisfy a demand for 90% confidence. (iv) Dispersion estimates for Rh/SiO_2 samples obtained through quantified IR spectra are in very good agreement with estimates obtained through hydrogen chemisorption experiments performed on other Rh/SiO_2 samples (*19*). (v) Linear and bridged carbonyl species exhibit approximately the same absorption intensities whether supported on silica or on alumina (*11*). (vi) The ratio of bridged CO to linear CO surface concentrations increased from approximately 0.2 to 0.5 as Rh dispersion decreased from 100 to 22%.

The general absence of any observed effect on absorption intensities by the factors studied in this research (Rh dispersion and temperature) is a fortunate result which may allow broader application of absorption intensity data than was previously thought possible. If the factors affecting absorption intensity values significantly can be identified and completely understood, quantitative FTIR can be used widely to determine surface concentations of CO and other species without the need for more calibration experiments.

RECOMMENDATIONS

Absorption intensities for CO on a wide variety of metals need to be determined. Preferably these studies will be conducted in a single laboratory with great attention paid to uniformity in preparation technique. The resulting data set will hopefully disclose more definite trends in absorption intensity as a fucntion of metal properties such as electronegativity or polarizability. Also, more research ought to be conducted on how various oxide supports effect absorption intensity values. This knowledge would be of great value if it led to a wider use of quantitative FTIR in the study of supported metal catalysts.

REFERENCES

1. Primet, M., El Azhar, M., Frety, R., and Guenin, M. *Appl. Catal.* **59,** 153 (1990).
2. Hecker, W. C., Wardinsky, M. D., Clemmer, P. G., and Breneman, R. B., *in* "Proceedings of the 9th International Congress on Catalysis, Calgary, 1988" (M. J. Phillips and M. Ternan, Eds.), p. 1106. The Chemical Institute of Canada, Ottawa, 1988.
3. Rasband, P. B., and Hecker, W. C., *Catal. Today,* **8,** 99 (1990).
4. Kaul, D. J., and Wolf, E. E., *J. Catal.* **89,** 348 (1984).
5. Yokomizo, G. H., Louis, C., and Bell, A. T., *J. Catal.* **120,** 1 (1989).
6. Winslow, P., and Bell, A. T., *J. Catal.* **86,** 158 (1984).
7. Levine, I. R., "Physical Chemistry," 3rd ed. McGraw–Hill, New York, 1988.
8. Seanor, D.A., and Amberg, C. H., *J. Chem. Phys.* **42,** 2967 (1965).
9. Vannice, M. A., and Twu, C. C., *J. Chem. Phys.* **75,** 5944 (1981).
10. Vannice, M. A., and Wang, S. Y., *J. Phys. Chem.* **85,** 2543 (1981).
11. Duncan, T. M., Yates, J. T. Jr., and Vaughan, R. W., *J. Chem. Phys.* **73,** 975 (1980).
12. Cant, N. W., and Donaldson, R. A., *J. Catal.* **78,** 461 (1982).
13. Shigeishi, R. A., and King, D. A., *Surf. Sci.* **58,** 379 (1976).
14. Cavanagh, R. R., and Yates, J. T. Jr., *J. Chem. Phys.* **74,** 4150 (1981).
15. Yates, J. T., Jr., Duncan, T. M., Worley, S. D., and Vaughan, R. W., *J. Chem. Phys.* **70,** 1219 (1979).
16. Hicks, R. F., Kellner, C. S., Savatsky, B. J., Hecker, W. C., and Bell, A. T., *J. Catal.* **71,** 216 (1981).
17. Rasband, P. B., M.S. thesis, Brigham Young University, 1991.
18. Rice, C. A., Worley, S. D., Curtis, C. W., Guin, J. A., and Tarrer, A. R. *J. Chem. Phys.* **74,** 6487 (1981).
19. Hecker, W. C. and Breneman, R. B., "Studies in Surface Science and Catalysis" (A. Crucq and A. Frennet, Eds.). Vol. 30, p. 257. Elsevier, Amsterdam, 1987.
20. Blyholder, G., *J. Phys. Chem.* **68,** 2772 (1964).
21. Davenport, J. W., *Chem. Phys. Lett.* **77,** 45 (1981).
22. Brown, T. L., and Darensbourg, D. J., *Inorg. Chem.* **6,** 971 (1967).
23. Walch, S. P., and Goddard, W. A. III, *J. Am. Chem. Soc.* **98,** 7908 (1976).